Thermal Conductance of Hydrophilic and Hydrophobic Interfaces

Zhenbin Ge, David G. Cahill, and Paul V. Braun

Department of Materials Science and Engineering, the Frederick Seitz Materials Research Laboratory, and the Beckman Institute for Advanced Science and Technology, University of Illinois, Urbana, Illinois 61801, USA

(Received 9 January 2006; published 8 May 2006)

Using time-domain thermoreflectance, we have measured the transport of thermally excited vibrational energy across planar interfaces between water and solids that have been chemically functionalized with a self-assembled monolayer (SAM). The Kapitza length—i.e., the thermal conductivity of water divided by the thermal conductance per unit area of the interface—is analogous to the "slip length" for water flowing tangentially past a solid surface. We find that the Kapitza length at hydrophobic interfaces (10–12 nm) is a factor of 2–3 larger than the Kapitza length at hydrophilic interfaces (3–6 nm). If a vapor layer is present at the hydrophobic interface, and this vapor layer has a thermal conductivity that is comparable to bulk water vapor, then our experimental results constrain the thickness of the vapor layer to be less than 0.25 nm.

DOI: 10.1103/PhysRevLett.96.186101 PACS numbers: 68.08.−p, 68.65.Ac

The structure and physical properties of interfaces between water and solid surfaces are critical inputs for understanding many microscopic processes in the biological and physical sciences, and for the design of new nanoscale systems [1–8]. At both hydrophilic and hydrophobic surfaces, the properties of water are modified in close proximity to the interface. For example, near hydrophilic surfaces, interfacial water has been found by computer simulation to have a higher density than in the bulk [2], while near hydrophobic surfaces, a thin layer of low-density water is predicted by theory [9–11] and has been observed in experiments [3,5,6,9,12]. Water confined between two hydrophobic surfaces is expected to spontaneously evaporate when the spacing between the surfaces is sufficiently small [13]. These differences in the structure of interfacial water are also revealed by measurements of rheological properties where strong violations of the no-slip boundary condition have been observed for fluid-flow tangential to hydrophobic interfaces [8,14].

Here we describe a new approach for probing the properties of interfacial water using measurements of the transport of thermal energy. Understanding this interface thermal conductance results in fundamental insights into the structure and properties of interfacial water and also has more practical implications. For example, biological systems contain both hydrophilic and hydrophobic surfaces [1,4]. Understanding the interfacial thermal conductance may enable a better understanding of thermal transport in thermally based medical therapies [15] that combine ultrafast lasers and metal nanoparticles as a source of heat.

The thermal conductance per unit area of the interface G is defined by $J = G\Delta T$, where J is the heat flux normal to the interface and ΔT is the temperature drop at the interface. The ratio of thermal conductivity divided by G can then be used to define the Kapitza length $h = \Lambda/G$, a characteristic length that gives the thickness of a layer with thermal conductivity Λ that has the same thermal resistance as the interface. As the characteristic dimensions of a system approach h, the interfacial thermal conductance plays an increasingly important role in thermal transport [16].

In our previous studies on G of solid-liquid interfaces, we employed colloidal dispersions of hydrophilic Au nanoparticles in aqueous solution [17,18]. The Au nanoparticles ranged in diameter from 3 to 24 nm and were functionalized with a wide variety of hydrophilic molecules; we determined G by modeling the cooling curves measured by transient absorption in an optical pump-probe experiment. In aqueous solution, despite the variety of surface chemistries we investigated, G was surprisingly constant, $150 < G < 250\ \mathrm{MW\,m^{-2}\,K^{-1}}$ [17], indicating that thermal coupling between hydrophilic surfaces and water is relatively strong regardless of the detailed chemistry. Because it is impossible to reliably suspend hydrophobic metal nanoparticles in aqueous solution—hydrophobic particles will rapidly aggregate—we could not answer an obvious next question: how do these values of G for hydrophilic interfaces compare with G for hydrophobic interfaces? Recently, we developed a means to measure G at planar interfaces by time-domain thermoreflectance [19,20], thereby enabling the study of interfaces between water and hydrophobic surfaces.

Two sample configurations were prepared as illustrated in Fig. 1 for studying Al and Au based interfaces. First, a 130 nm thick film of SiO_2 was deposited by e-beam evaporation on the bottom of a sapphire substrate. This layer serves as an antireflection optical coating at 770 nm, the laser wavelength used in the pump-probe measurements. A polyimide precursor was spin coated on the top of the sapphire substrate and cured at 250 °C in air, resulting in a 20–30 nm thick layer with low thermal conductivity; this layer ensures that most of the heat deposited in the overlying metal film flows into the liquid at short time scales, maximizing the sensitivity of our experiment to the thermal conductance of the solid-liquid interface. Different

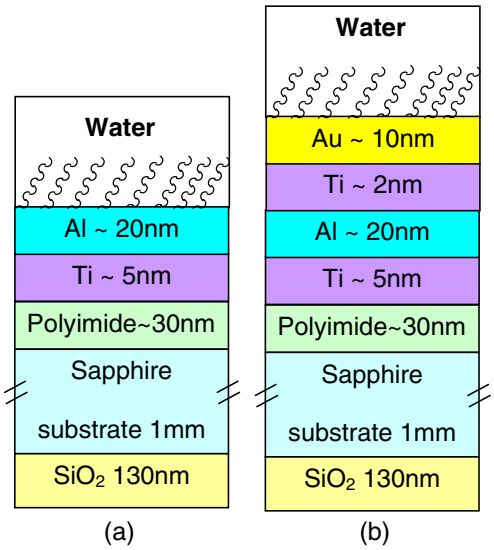

FIG. 1 (color online). Schematic of sample structures for studying (a) aluminum-water interface thermal conductance; (b) gold-water interface thermal conductance.

combinations of Ti, Al, and Au were then deposited on the polyimide films by sputtering. Ti layers, 2–5 nm thick, serve as adhesion layers and the 20–30 nm Al layer provides a sensitive thermometer in the experiment through its relatively large thermoreflectance at optical wavelengths near 770 nm. This Al layer can be directly modified with silane molecules [Fig. 1(a)], or can be coated by Ti, followed by 10–20 nm of Au, and subsequently modified with well-known gold-thiol chemistry [Fig. 1(b)] [21].

We study both Al and Au based interfaces because Al and Au offer complementary strengths and weaknesses for our experiments. Molecular monolayers formed using thiol chemistry on Au are better understood and probably more homogeneous than layers formed by silane chemistry on the native oxide of Al but the Au layer introduces an additional thermal resistances between the Al thermometer and the interfaces with water that we are most interested in studying. Near an interface with a nonmetal, the relatively weak electron-phonon coupling in Au results in a non-negligible thermal resistance [22,23]. Therefore, the thermal conductance of an interface with Au includes an additional conductance G_{ep} in series: $G_{ep} = \sqrt{g\Lambda}$, where g describes the conductance per unit volume of the coupling between electrons and phonons in Au; and Λ is the lattice thermal conductivity of Au. Using $\Lambda = 2.7\ \mathrm{W\,m^{-1}\,K^{-1}}$ [24]; $g = 3.1 \times 10^{16}\ \mathrm{W\,m^{-3}\,K^{-1}}$ [25], gives $G_{ep} = 290\ \mathrm{MW\,m^{-2}\,K^{-1}}$. For Al, both g and Λ are much larger than for Au [$g = 4.9 \times 10^{17}\ \mathrm{W\,m^{-3}\,K^{-1}}$ [26]; $\Lambda = 10\ \mathrm{W\,m^{-1}\,K^{-1}}$ [27]], and $G_{ep} > 2\ \mathrm{GW\,m^{-2}\,K^{-1}}$. Also, the interface between the Au and Al layers introduces a measurable thermal resistance, presumably because of contamination of the Ti adhesion layer by residual gases in the deposition chamber. The conductance of the Al/Ti/Au interfaces is measured separately by fitting the data at short delay times of less than 100 ps; this additional interface conductance does not produce a significant change in the measurement of the water interfaces but this effect is included in the thermal model for samples containing Au.

Octadecyltrichlorosilane (OTS) was used to functionalize the native oxide of the Al surface making it hydrophobic. The advancing water contact angle is $\theta_{adv} = 104°$ and the receding water contact angle is $\theta_{rec} = 90°$; the thickness of the self-assembled monolayer (SAM) measured by ellipsometry, using an index of refraction $n = 1.45$, is 2.4 ± 0.3 nm. 2-[methoxy(polyethyleneoxy)-propyl]-trichlorosilane (PEG-silane) was used to make the Al surface hydrophilic [28]. The water contact angles are $\theta_{adv} = 16°$ and $\theta_{rec} = 13°$; the SAM thickness is 0.7 ± 0.2 nm. The Au surface was functionalized with 1-octadecanethiol (C_{18}) making it hydrophobic. The water contact angles are $\theta_{adv} = 103°$ and $\theta_{rec} = 94°$; the SAM thickness is 2.3 ± 0.3 nm. 11-mercapto-1-undecanol ($C_{11}OH$) was used to functionalize the Au surface making it hydrophilic [21]. The water contact angles are $\theta_{adv} = 18°$ and $\theta_{rec} = 9°$; the SAM thickness is 1.1 ± 0.2 nm.

The thermal conductance of the interfaces with water was measured using time-domain thermoreflectance [19,20]. Two thermal models were used to analyze the raw data: unidirectional heat flow was used to analyze the heat transfer when the metal surface was exposed to air, and bidirectional heat flow was used to analyze the heat transfer when the metal surface was immersed in water [29]. Metal film thicknesses are measured by Rutherford backscattering spectrometry, as shown in Fig. 2; heat capacities are taken from literature values. The thermal conductivity of the polyimide film was separately measured to be $0.17\ \mathrm{W\,m^{-1}\,K^{-1}}$ using an Al/polyimide/Si stack; the thickness of the polyimide film is adjusted in the unidirectional heat flow model to obtain the best fit between the model and the data. The bidirectional thermal model then has only one remaining free parameter, G, the thermal conductance of metal-water interface, that we adjust to obtain the best fit. Because the thermal diffusivities of water and polyimide are small, heat flow in these experiments is primarily one dimensional; however, both of thermal models take into account the full three-dimensional heat flow in cylindrical coordinates [29,30].

Examples of time-domain thermoreflectance data and fits are shown in Fig. 3 for hydrophobic and hydrophilic Al-water and Au-water interfaces. Oscillations observed in the short time region are the result of longitudinal acoustic oscillations of the metal films. G for the OTS modified hydrophobic Al surface in water is determined to be $60 \pm 5\ \mathrm{MW\,m^{-2}\,K^{-1}}$ and G for C_{18} modified hydrophobic Au surface in water is $50 \pm 5\ \mathrm{MW\,m^{-2}\,K^{-1}}$. The hydrophilic surfaces resulted in significant increase in G. G of the PEG-Silane modified Al surface in water is $180 \pm 30\ \mathrm{MW\,m^{-2}\,K^{-1}}$, and G of $C_{11}OH$ modified hydrophilic Au surface in water is $100 \pm 20\ \mathrm{MW\,m^{-2}\,K^{-1}}$.

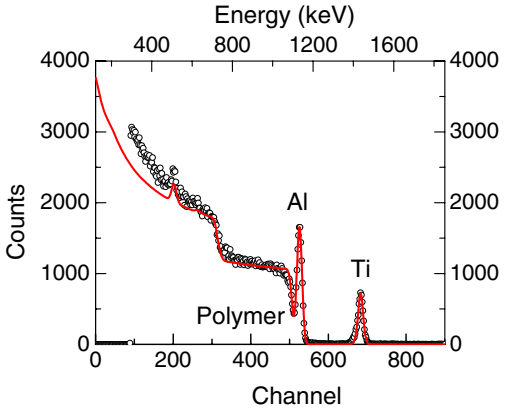

FIG. 2 (color online). Rutherford backscattering spectrometry data for determining metal film thicknesses of the samples. Open circles are measured intensities. Solid line is a fit using SIMNRA 5.02 with polymer and metal thicknesses as the free parameters. For this particular sample, the Ti thickness is 5.3 nm and Al thickness is 34.0 nm. The depth of the valley between the Al in the thin film and the Al in the sapphire substrate is determined by the thickness of polymer.

These results for planar hydrophilic functionalized Al and Au surfaces are in good agreement with our previous work using Au nanoparticles in aqueous solution [17,18]. Both sets of experiments give G ranging between 100 and 300 MW m^{-2} K^{-1} indicating that the thermal coupling between hydrophilic surfaces and water is strong regardless of whether the surfaces are nanoparticles or planar films.

Our experimental values for G at hydrophilic interfaces are smaller by a factor of approximately 2 than the results of molecular dynamics (MD) simulations of interfaces between water and the hydrophilic head group ($-$OH) of a surfactant molecule; these simulations found $G =$ 300 MW m^{-2} K^{-1} [31]. The authors of Ref. [31] attributed the large thermal conductance to the strong coupling of water molecules with the hydroxyl head of the surfactant molecules by hydrogen bonding. The smaller value for G in our experiments on Au-C_{11}OH/water interface compared to Al-PEG/water may be due to the issues of electron-phonon coupling in Au described above: since we estimate $G_{ep} = 290$ MW m^{-2}K^{-1}, the conductance of the lattice vibrations at the interface may, in fact, be close to $G = 150$ MW m^{-2} K^{-1}, i.e., nearly identical to our measured value for the Al-PEG/water interface.

We are not aware of any MD simulations of the thermal conductance across an interface between water and a solid hydrophobic surface. The closest case is a water-octane interface, in which $G = 65$ MW m^{-2} K^{-1} [31]. This is similar to our results on hydrophobic-water interfaces, but additional simulations that include the long-range van der Waals attractions [32] will be helpful in identifying the microscopic mechanisms that control thermal transport across hydrophobic interfaces.

Even if we neglect the issues of electron-phonon coupling, i.e., the finite value of G_{ep}, the value of the interface conductance that we measure includes 4 processes: (i) flow of heat from metal films to functional groups (i.e., S or Si group), (ii) flow of vibrational energy along the length of the molecular chain, (iii) transport of vibrational energy

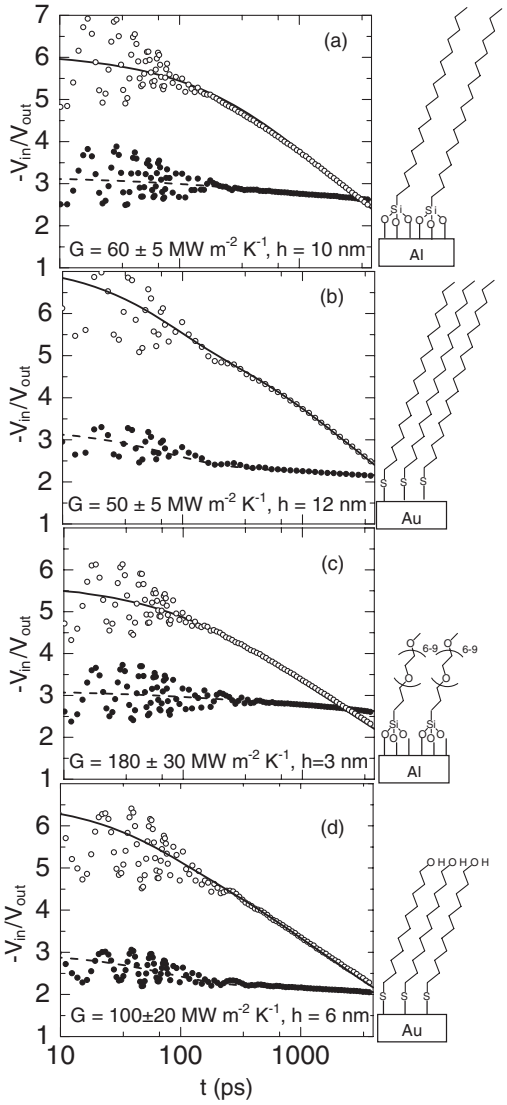

FIG. 3. Time-domain thermoreflectance data for thermal transport across hydrophobic (a), (b) and hydrophilic (c), (d) metal-water interfaces. The ratio of the in-phase to out-of-phase signals of the lock-in amplifier is plotted as a function of the delay time t between pump and probe. Solid circles, dry state; open circles, in water. Dashed lines are fits based on the unidirectional model with the polyimide thickness as the one free parameter (heat dissipated through air is negligible). Solid lines are fits based on the bidirectional model (heat is dissipated through both water and the polyimide layer) with the solid-liquid interface thermal conductance, G, as the one free parameter. (a) OTS modified Al surface, hydrophobic, $G = 60 \pm 5$ MW m^{-2} K^{-1}, Kapitza length $h = 10$ nm; (b) C_{18} modified Au surface, hydrophobic, $G = 50 \pm 5$ MW m^{-2} K^{-1}, $h = 12$ nm; (c) PEG-silane modified Al surface, hydrophilic, $G = 180 \pm 30$ MW m^{-2} K^{-1}, $h =$ 3 nm; (d) C_{11}OH modified Au surface, hydrophilic, $G = 100 \pm$ 20 MW m^{-2}K^{-1}, $h = 6$ nm.

from the terminal group to the contacting, possibly low density, surrounding water, and (iv) flow of heat across the possibly low-density water gap to the bulk water phase. Because well-aligned polyethylene has a high thermal conductivity, 30 times higher than water [33], the temperature drop along the molecular chains, i.e., process (ii), is probably not significant. The large difference between G for hydrophilic and hydrophobic interfaces suggests that the third and/or fourth mechanism(s) play a critical role in thermal transport across hydrophobic interfaces.

The difference in the Kapitza lengths of hydrophobic and hydrophilic interfaces places constraints on the thickness of a possible vapor layer at hydrophobic interfaces. The existence of a nm-scale water-vapor layer at hydrophobic interfaces, or, in other words, the degree of ''drying'' of a hydrophobic interface, has been controversial for many years [1,32]. If we can assume that the thermal conductivity of the vapor layer has the same thermal conductivity as bulk water-vapor, approximately 30 times smaller than water, then the thickness of this vapor layer must be less than $\Delta h/30 = 0.25$ nm, where Δh is the difference in the Kapitza lengths for hydrophilic and hydrophobic interfaces. Recently, neutron diffraction experiments on the structure of interfacial water near hydrophobic interfaces were modeled by an error function of width σ and a midpoint shifted by a distance δ from the hydrocarbon-water interface; for naturally aerated heavy water, $\sigma \sim 0.35$ nm and $\delta \sim 1.0$ nm and the offset was as small as $\delta = 0.2$ nm in heavy-water bubbled by Ar to remove dissolved gases [3]. We, however, did not observe significant changes in the thermal conductance when we used Ar-bubbled deionized water instead of the deionized water directly from a mili-Q dispenser, or when we used water degassed in vacuum overnight.

The slip length in fluid flow past a hydrophobic surface has also been controversial and no consensus has emerged on the value of the slip length in the limit of small shear rates or how the slip length varies with shear rate [8,14,34]. Surface morphology is thought to play an important role in the rheology experiments because fluid flow tangential to a surface can be strongly modified by a low density of protrusions [14]. In this regard, measurements of the interface thermal conductance may be much less sensitive to the perfection of the experimental system, and therefore, more easily interpreted in terms of intrinsic mechanisms.

Through this work, we establish the interface thermal conductance G for hydrophilic and hydrophobic surfaces (Fig. 3). The smallest conductance for hydrophobic-water interfaces measured to date is 50 $\mathrm{MW\,m^{-2}\,K^{-1}}$, with a Kapitza length, $h = \Lambda/G = 12$ nm. This large thermal resistance might be a significant factor modulating heat flow in biological systems as well as nanoscale systems that contain high densities of hydrophobic interfaces [31].

This work was supported by US DOE Grant No. DEFG02-01ER45938 and the WaterCAMPWS under NSF Agreement No. CTS-0120978. Rutherford backscattering spectrometry was carried out in the Center for Microanalysis of Materials, University of Illinois, which is partially supported by the US Department of Energy under Grant No. DEFG02-91-ER45439.

[1] P. Ball, Nature (London) **423**, 25 (2003).
[2] G. Cicero *et al.*, J. Am. Chem. Soc. **127**, 6830 (2005).
[3] D. A. Doshi *et al.*, Proc. Natl. Acad. Sci. U.S.A. **102**, 9458 (2005).
[4] J. Israelachvili and H. Wennerstrom, Nature (London) **379**, 219 (1996).
[5] D. Schwendel *et al.*, Langmuir **19**, 2284 (2003).
[6] R. Steitz *et al.*, Langmuir **19**, 2409 (2003).
[7] X. Y. Zhang, Y. X. Zhu, and S. Granick, Science **295**, 663 (2002).
[8] Y. X. Zhu and S. Granick, Phys. Rev. Lett. **87**, 096104 (2001).
[9] K. Lum, D. Chandler, and J. D. Weeks, J. Phys. Chem. B **103**, 4570 (1999).
[10] F. H. Stillinger, J. Solution Chem. **2**, 141 (1973).
[11] J. D. Weeks, Annu. Rev. Phys. Chem. **53**, 533 (2002).
[12] U. K. Sur and V. Lakshminarayanan, J. Colloid Interface Sci. **254**, 410 (2002).
[13] A. Luzar, J. Phys. Chem. B **108**, 19 859 (2004).
[14] C. Cottin-Bizonne *et al.*, Phys. Rev. Lett. **94**, 056102 (2005).
[15] L. R. Hirsch *et al.*, Proc. Natl. Acad. Sci. U.S.A. **100**, 13 549 (2003).
[16] D. G. Cahill *et al.*, J. Appl. Phys. **93**, 793 (2003).
[17] Z. B. Ge, D. G. Cahill, and P. V. Braun, J. Phys. Chem. B **108**, 18 870 (2004).
[18] O. M. Wilson *et al.*, Phys. Rev. B **66**, 224301 (2002).
[19] R. M. Costescu, M. A. Wall, and D. G. Cahill, Phys. Rev. B **67**, 054302 (2003).
[20] C. A. Paddock and G. L. Eesley, J. Appl. Phys. **60**, 285 (1986).
[21] C. D. Bain *et al.*, J. Am. Chem. Soc. **111**, 321 (1989).
[22] A. Majumdar and P. Reddy, Appl. Phys. Lett. **84**, 4768 (2004).
[23] Y. S. Ju, J. Heat Transfer **127**, 1400 (2005).
[24] G. K. White, S. B. Woods, and M. T. Elford, Philos. Mag. **4**, 688 (1959).
[25] J. H. Hodak, A. Henglein, and G. V. Hartland, J. Chem. Phys. **112**, 5942 (2000).
[26] G. Tas and H. J. Maris, Phys. Rev. B **49**, 15 046 (1994).
[27] R. J. Gripshover, J. B. Vanzytveld, and J. Bass, Phys. Rev. **163**, 598 (1967).
[28] N. Tillman *et al.*, J. Am. Chem. Soc. **110**, 6136 (1988).
[29] D. G. Cahill, Rev. Sci. Instrum. **75**, 5119 (2004).
[30] A. Feldman, High Temp. High Press. **31**, 293 (1999).
[31] H. A. Patel, S. Garde, and P. Keblinski, Nano Lett. **5**, 2225 (2005).
[32] D. Chandler, Nature (London) **437**, 640 (2005).
[33] D. B. Mergenthaler *et al.*, Macromolecules **25**, 3500 (1992).
[34] C. H. Choi, K. J. A. Westin, and K. S. Breuer, Phys. Fluids **15**, 2897 (2003).